JOURNAL OF PROPULSION AND POWER
Vol. 17, No. 6, November–December 2001

Two-Stage-to-Orbit Spaceplane Concept with Growth Potential

Unmeel B. Mehta* and Jeffrey V. Bowles†
NASA Ames Research Center, Moffett Field, California 94035

A two-stage-to-orbit (TSTO) spaceplane concept developed in 1993 is revisited, and new information is provided to assist in the development of the next-generation space transportation vehicles. The design philosophy, TSTO spaceplane concept, and the design method are briefly described. A trade study between cold and hot structures leads to the choice of cold structures with external thermal protection systems. The optimal Mach number for staging the second stage of the TSTO spaceplane (with airbreathing propulsion on the first stage) is 10, based on life-cycle cost analysis. Mass properties of four TSTO spaceplanes with a turbo/ram/scramjet propulsion system on the first stage are presented, and the specification and performance of one of these spaceplanes are discussed. Two of these spaceplanes have builtin growth potential, and one of these is proposed as a prototype/experimental TSTO spaceplane to address the near-term access to space needs. The internal rate of return on investment is the highest for the proposed TSTO spaceplane, vis-à-vis a single-stage-to-orbit rocket vehicle and a TSTO spaceplane without builtin growth. Additional growth potentials for the proposed spaceplane are suggested. This spaceplane can substantially decrease access-to-space cost and risk and increase safety and reliability in the near term. It can be a serious candidate for the next-generation space transportation system.

Introduction

IN 1959, the request for recoverable booster system, with a goal of routine access to space, led to the recoverable orbital launch system (aerospace plane) program in the United States.[1] The U.S. Air Force emphasized two-stage-to-orbit (TSTO) concepts as first-generation options, based on guidance from the Air Force Scientific Advisory Board and other ad hoc committees. In November 1965, after intensive study, review, and evaluation, the TSTO approach (airbreathing first stage with a conventional rocket second stage) was selected as the preferred approach. In 1970, when the U.S. Space Shuttle Phase B award began, NASA and contractors were generally unanimous in considering TSTO fully reusable vehicles as the vehicle of choice.[2] In 1993, the Rand Corporation believed that the 1965 choice by the U.S. Air Force was commendable and that it would be a strong contender for developing the X-30 spaceplane under the National Aerospace Plane (NASP) program.[1] In 1993, after reviewing the status of X-30, the U.S. General Accounting Office recommended a reexamination of the worth of pursing single-stage-to-orbit (SSTO) on its own merit.[3] In 1994, Rich expressed that Orient Express (X-30) is actually two separate concepts, one a rocketship and the other an airplane.[4] "Most likely, that particular twain shall never meet successfully."[4] Based on state-of-the-art hypersonic technologies,[3,5,6] the SSTO concept is an extreme technical challenge, and its commercial viability is highly questionable in the near term. Nevertheless, the SSTO concept is still advocated.[7]

Today, the choice of TSTO concept as the near-term option appears to be the correct one. In 1993, a spaceplane based on the TSTO concept was conceptualized for the Access to Space—Advanced Technology Team.[8] This spaceplane is briefly described in Ref. 9. A strategy for developing airbreathing spaceplanes, using a TSTO spaceplane concept, is presented in Ref. 10. Essential aspects of this concept and of this strategy are revisited, and additional information, some based on subsequent work, is provided herein for consideration to assist in the development of next-generation spaceplanes.

Received 2 January 2001; revision received 11 April 2001; accepted for publication 11 April 2001.

*Division Scientist, Space Technology Division, Mail Stop 229-3. Associate Fellow AIAA.

†Aerospace Engineer, Systems Analysis Branch, Mail Stop 258-1.

The lessons drawn from past programs suggest the following design philosophy for the development of the next-generation space transportation system[10]: 1) technology-driven development, 2) short-term economical benefits, 3) growth potential, 4) achievable, and 5) safe and reliable, even at the expense of greater up-front cost and lower performance. The economical benefits are judged for commercialization of space transportation. By definition, a commercial venture is a low-risk investment and generates a 20+% return per annum on investment with the investment payback (preferably) within 5 years. The design philosophy and economics requirement lead to a spaceplane concept based on two stages, to a spaceplane that operates like an aircraft and to a spaceplane design with builtin growth potential.

Staging can increase performance of a given technology, reduce the vehicle sensitivity to performance parameter variations, or deliver equal performance and lower risk with less advanced technology. TSTO vehicles offer greater margin and have higher payload potential than SSTO vehicles for a given takeoff gross weight (TOGW). TSTO vehicles require smaller propellant mass fractions, resulting in lower TOGW than SSTO vehicles for a given payload mass. TSTO vehicles require propellant mass fractions that are easier to achieve than those for SSTO vehicles. If vehicles with airbreathing propulsion are considered, first stages of a TSTO concept have potential for greater atmospheric-cruise capability than SSTO vehicles, and the operational airbreathing corridor for TSTO vehicles can be larger than that for SSTO vehicles.

The hypersonic, airbreathing corridor (in terms of dynamic pressure) is bounded on one side by the limits on structural forces, aeroheating environments, and the integrated drag loss on the vehicle and on the other side by combustor pressure requirements and by the planform area required for sustained flight. Accelerators to orbit fly along the trajectory of their highest allowable dynamic pressure to maintain sufficient engine thrust margin and, thus, sufficient acceleration. Accelerators have much bigger inlet area relative to body cross section than hypersonic cruisers. For cruisers, the task is to maximize Breguet range and configuration lift-to-drag ratio at the design point. The heating rate impacts the structure of the accelerator, whereas the integrated heat load is the concern for cruiser. Consequently, accelerators fly at dynamic pressures close to 2100 lbf/ft^2, whereas, cruisers fly at dynamic pressures near 600 lbf/ft^2. A dual-use first stage of a TSTO vehicle, capable of performing as an accelerator and as a cruiser, can operate in a wider airbreathing corridor than an airbreathing-powered SSTO accelerator. The latter vehicle is difficult to design because the required propellant mass fraction is very

difficult to achieve. To design a dual-use SSTO vehicle would be certainly much more difficult.

The need for developing two stages is of a secondary consideration to the aforementioned design philosophy, economic requirement, and advantages over SSTO vehicles.

Orbital-mission flexibility and greatly enhanced operability are achievable if spaceplanes have features that approach those of commercial aircraft. Airbreathing propulsion provides higher overall performance and far greater operability than that possible with rocket propulsion. Examples of enhanced operability with turbine-based combined or combination cycle (TBCC) propulsion on the first stage of a TSTO vehicle are aircraftlike operations, including powered-landing, go-around, in-flight refueling, ferrying, and, at low speed, vehicle intact-abort capability. Aircraftlike capabilities are difficult or impossible to achieve with rocket propulsion, air-augmented rocket propulsion, and with rocket-based combined or combination cycle (RBCC) propulsion. The TBCC propulsion concept has significant advantage, primarily because it offers the highest specific impulse at low speed and the most vehicle controllability. Consequently, the TBCC engine has a distinct advantage whenever the vehicle design is driven by safety.

An RBCC engine with a scramjet cycle on the second of a TSTO spaceplane offers an advantage over a rocket-powered second stage. The significance of the advantage increases as the operational Mach number range of the scramjet engine is extended.

In addition to the aforementioned attributes of a TSTO spaceplane with a TBCC engine on the first stage, the full reusability of spaceplanes leads to significantly reduced operational costs, which in turn, reduce the life-cycle costs (a sum of development, acquisition, and operation costs) of a fleet of spaceplanes. If spaceplanes are designed with built in growth, life-cycle costs are further reduced. The TSTO spaceplane, with airbreathing propulsion on the first stage, can fulfill the near-term access-to-space goals, while greatly reducing the cost, substantially improving mission flexibility, operability, safety, and reliability, and offering significant growth potentials and multiple avenues.

TSTO Spaceplane Concept

Figure 1 shows an artist's rendition of the TSTO spaceplane considered for the mission of achieving 220 mile circular orbit at a 51.6-deg inclination, with 25,000-lb payload [International Space Station (ISS) resupply mission]. The genesis of this spaceplane is Ref. 11 issued by Lockheed Company in 1967 for NASA Ames Research Center.[11]

Both the first stage (launcher) and second stage (orbiter) vehicles are lifting-body configurations. The orbiter is nestled within the outer mold line of the launcher. The cargo bay dimensions of the orbiter are $15 \times 15 \times 30$ ft. The launcher propulsion system consists of a turbo/ram/scramjet propulsion system, including low- and high-speed airbreathing engines, whereas the orbiter propulsion system is a conventional liquid oxygen (LOX)/hydrogen rocket engine.

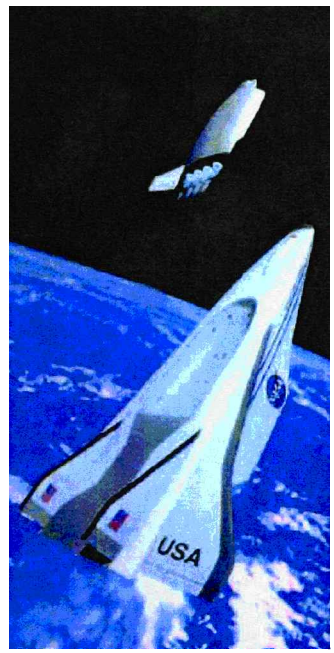

Fig. 1 Artist's rendition of the TSTO spaceplane concept.[8]

The structural concept for the launcher and orbiter is cold-structure, skin-stringer/frame-stiffened, integral-lobed tanks (aluminum–lithium alloy for LOX tank and composite for hydrogen tank), with composite intertank structure. The external thermal protection system (TPS) consists of advanced ceramic tile/blanket systems. Both stages of the spaceplane are designed with 15% dry-weight margin.

Each stage of the spaceplane has a crew of two. The launcher takes off horizontally and both stages land horizontally, with the launcher making a powered landing. The takeoff speed is limited to 300 kn. Staging is executed at low hypersonic Mach number ($5 < M \leq 12$). The maximum axial acceleration during ascent is limited to 3.0 g, and the normal load factor is limited to 2.5 g.

After launching the orbiter, the launcher executes a decelerating 180-deg turn and cruises on the low-speed airbreathing system back to the launch site. After separation, the orbiter continues to accelerate up to main engine cutoff (MECO), coasts to the target apogee, and circularizes at that altitude. Herein, the orbiter is designed to have an onorbit reserve ΔV of 600 ft/s, which is approximately 2% of the total ΔV to orbit. After completing the onorbit mission, the orbiter deorbits, enters the atmosphere, decelerates aerodynamically while banking to meet cross-range requirements, and executes an unpowered landing at the launch base.

A study was conducted to determine the extent to which the orbiter is submerged within the launcher. Structural depth of the launcher in the payload region is traded for transonic drag increment of the mated combination. The lowest weight system resulted when the orbiter was fully submerged.

Hydrogen is the preferred fuel for the launcher for a number of reasons. First, hydrogen offers significant propulsion efficiency and thermal cooling capability over hydrocarbons, resulting in lower weights and costs. Second, the sizing of the hydrocarbon-powered launcher is principally determined by the size of the orbiter, whereas the size of the hydrogen-powered launcher is mainly determined by its fuel-fraction mission requirements. In the latter case, the possibility of forming hydrogen onboard from hydrocarbons and water is not considered. If it were considered, the onboard hydrogen generation[12] would also impact the sizing of the launcher. Third, hydrocarbons limit the launcher performance growth. Fourth, the staging Mach number can be higher with hydrogen than with hydrocarbons. Finally, there is little risk avoidance provided by hydrocarbons on the launcher if hydrogen is used on the orbiter.

Hydrogen-powered, afterburning turbojets were selected for the launcher low-speed propulsion system. Figure 2 shows the jet engines installed on the launcher, consisting of an over-and-under arrangement of turbojets and ram/scramjets. As a function of flight Mach number, the inlet splitter plate position is set to provide the turbojet engine the required inlet mass flow. The turbojet engine sea-level thrust level is in the 70,000-lb class. Six turbojet engines are installed; they are used from Mach 0 to 3.0, including takeoff and transonic acceleration. The weight of the turbojet system includes bare engine weight, afterburner and nozzle weight, and the close-off door, resulting in an installed engine sea-level thrust-to-weight ratio of 6.65. The operating range of turbojet engines

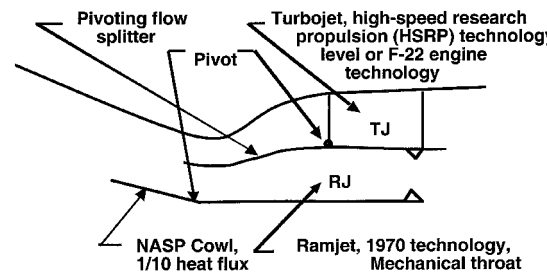

Fig. 2 Jet engines installation.[9]

Table 1 HAVOC aerodynamics

Parameters	Subsonic	Transonic	Supersonic and Hypersonic
Lift			
Body		Empirical f (AR, Mach)	Tangent wedge/Tangent cone Newtonian Mach > 18
Wing		Low AR theory	Linearized supersonic
Drag			
Induced		Empirical f (Mach)	Tangent wedge/Tangent cone Newtonian Mach > 18
Skin friction		Schlichting	Reference enthalpy Eckert, Van Driest, Schlichting Re_θ/M (transition criteria)
Body wave	0	Empirical f (mean sweep, FR, Mach)	Tangent wedge/Tangent cone Newtonian Mach > 18
Wing wave	0	Empirical f (sweep, T/C)	Prandtl–Meyer Shock expansion
Bluntness	0	0	Leading-edge radius/Sweep and Newtonian
Base		Empirical f (Mach)	70% Vacuum

AR: Aspect Ratio, FR: Fineness Ratio.

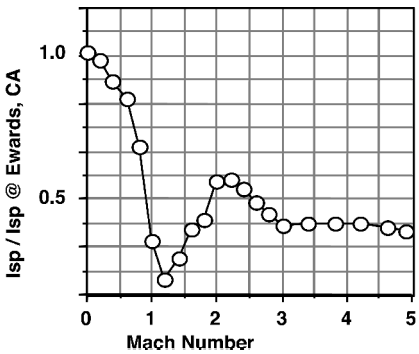

Fig. 3 Launcher propulsion specific impulse.

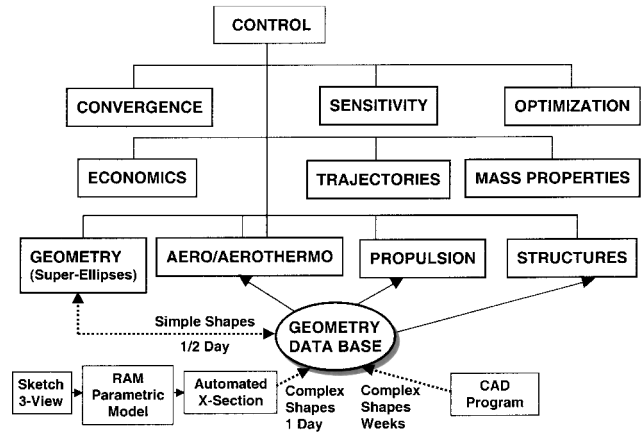

Fig. 4 Hypersonic aerospace vehicle optimization code (HAVOC).

could be extended to Mach 3.5, with present, state-of-the-artturbojet technology.

The ramjet is started at Mach 1.05, to cancel ram drag and internal friction, and operated to 6.0. Base burning is initiated at Mach 0.5 and terminated at Mach 2.5. Principally, from Mach 0.9 to 1.4, base burning is used to reduce transonic nozzle drag. At the transonic pinch point, the resultant acceleration is 2.3 ft/s^2. The reduced transonic specific impulse I_{sp}, shown in Fig. 3, reflects the fuel consumed for base burning. Transitioning from ramjet mode above Mach 6, the NASP-derived, dual-mode, ram/scramjet engine technology is used.

The orbiter propulsion system consists of main rocket engines and an integrated orbital maneuver system/reaction control system (OMS/RCS) system. The baseline OMS/RCS system is a liquid H_2/O_2-fueled system. The main rocket engines are H_2/LOX engines, based on RL-10 technology with vacuum and sea-level specific impulse of 446 and 362 s, respectively. The thrust class of the engine is approximately 150,000 lb, with an engine thrust-to-weight ratio of 54. It was well within 1993 technology limits and is similar to the Pratt and Whitney RL2000-study engine. Four engines are selected to provide abort-to-orbit capability from the launch point, if an engine is shut down. From Mach 5-launch condition, the orbiter can attain an orbit altitude of 65 n mile, which is sufficient to return to the launch site on the next orbital pass.

A low-pressure, expansion-cycle rocket engine is used due to its simple architecture, which would result in high operational reliability and maintainability and in relatively low development and acquisition costs. In fact, the orbiter could use any of the advanced rocket engines, such as an advanced-staged, combustion-cycle engine, modular engines, aerospike engines, etc. The payload capabilities of the orbiter could be enhanced with these advanced, higher-performance, lower-weight engine systems.

Analysis Method

The NASA Ames Research Center developed hypersonic aerospace vehicle optimization code (HAVOC) for hypersonic vehicle synthesis is used to perform estimates of systems performance characteristics and design specifications (Fig. 4). It uses engineering analysis methods to compute vehicle performance and design characteristics, including aero- and thermodynamics, propulsion, structures, trajectory, and system cost. In the design process, the synthesis code closes the design to meet mission performance requirements, matching vehicle weight and volume required to that available.

Aero- and Thermodynamics

The subsonic and transonic aerodynamics for a given configuration are computed as functions of the freestream Mach number, angle of attack, and the gross geometric parameters of the body and wing (Table 1). Experimental or high-fidelity computational results are used to calibrate the empirical methods in the low-speed regime for the body, including the high-subsonic/transonic/low-supersonic base drag model. In the supersonic/hypersonic speed range, the fuselage pressure and aerodynamic forces (lift and pressure drag) are computed using real-gas tangent-wedge/tangent-cone, independent-panel methods. For the higher hypersonic Mach number regime, Newtonian methods are used to compute surface-pressure coefficients. Friction drag is computed using various reference enthalpy methods, for example, Eckert or van Driest. The engine-off base drag is computed using empirical relations for the high-subsonic/transonic/low-supersonic speed range and is estimated at higher Mach numbers assuming a 70% vacuum in the base region, that is, $Cp_{\text{base}} = -1/M^2$.

Calculation of the aerothermal environment begins with the flight condition along the vehicle trajectory. With the flight condition specified, that is, given the freestream Mach number, the angle of attack, and the freestream dynamic pressure, the boundary-layer edge conditions are computed for each panel. For acreage-heating calculations, the skin-friction coefficient is computed using reference enthalpy methods noted earlier.

Calculations of local skin friction and convective heat transfer film coefficient involve an iteration to balance the convective heat flux, the radiative heat flux, and the conductive heat flux into the vehicle. For vehicle designs with exterior insulation, the thermal

energy conducted into the TPS is generally on the order of 5% of the total convective heating. Neglecting this relatively small conduction term in the surface energy balance results in a somewhat higher radiation equilibrium surface temperature, which is used as a design margin for the TPS. The reference Reynolds number is then computed using the boundary-layer edge velocity determined earlier and the running length for that panel location. The local skin-friction coefficients and local Stanton numbers are then calculated using the Reynolds analogy and the reference Prandtl number with the appropriate formulation, depending on laminar or turbulent flow conditions. Finally, the convective heating film coefficient is computed from the Stanton number, reference density, and edge velocity.

The local recovery enthalpy is determined using the edge static enthalpy, the edge velocity, and the edge Prandtl number, with the Prandtl number correction factor for laminar or fully turbulent flow, as appropriate. The convective heat-flux rate is then computed.

The radiative heat flux is computed by determining the emissivity as a function of TPS material distribution and the wall temperature. The iteration loop is repeated until surface energy balance is achieved.

For blunt, leading-edge heating calculations, a modified stagnation heating Faye-Ridell method[13] is used. The hot-wall heating rate is computed for off-stagnation conditions using a modified Lee's method.[14] The stagnation point is determined using a Newtonian model with the unit surface normal collinear with the freestream velocity vector. The actual wall temperature computed for stagnation regions, or acreage areas, will generally differ from the radiation equilibrium wall temperature computed earlier. This conducting wall temperature depends on the heating history along the trajectory. Up to the peak-heating point, heat is conducted into the TPS, and the resulting wall temperature will be lower than the nonconducting wall temperature. After peak heating, the TPS begins to reject heat, with the resulting conductive heat flux back to the surface resulting in a higher wall temperature than the nonconducting value.

Propulsion

For the rocket engine, a simplified performance model is used, with vacuum and sea-level-specific impulse as inputs, along with vacuum thrust. Altitude performance of the rocket is computed using ambient pressure corrections to I_{sp}.

For the ramjet, dual-mode and scramjet operation, a nose-to-tail propulsion model uses the keelline geometry and quasi-one-dimensional area distribution of the combustor to compute the propulsion flowfield. This nose-to-tail propulsion model consists of a planar inviscid two-dimensional real-gas, weak-wave flow code, coupled to a one-dimensional subsonic/supersonic combustor analysis code, to predict nose-to-tail flow-path characteristics. The forebody boundary layer is computed using the inviscid solution to provide edge conditions. Shear forces and heat transfer are computed for the forebody/inlet using reference enthalpy methods. Inlet unstart and self-start boundaries are computed using computed flowfield properties at the cowl-lip plane, and one-dimensional isentropic flow between the cowl lip and inlet throat.

Beginning at the inlet throat, the one-dimensional combustor mass, momentum, and energy equations with wall skin friction and heat transfer are solved (stepwise) through the cumbustor. Multiple fuel-injector stations and preburning are provided for. Combustor efficiency, that is, heat-release schedule, is computed as a function of injector Mach number and injection angle, local equivalence ratio, and axial distance from injector station. Overall engine heat balance is computed using an input combustor, skin-friction coefficient as a function of freestream Mach number.

In dual-mode operation, normal shock and thermal choke plane locations are also computed. The nozzle flowfield is then computed from the combustor exit solution using the real-gas, weak-wave two-dimensional code, which includes nozzle and cowl-flap geometry. Equilibrium or frozen flow is computed in the nozzle region using the mole fraction array at the combustor exit plane. First-order estimates of axial and normal forces and of pitching moments are computed as a function of vehicle geometry and flight conditions. Overall propulsion system heat loads are then used to determine fuel inlet total temperature or to compute required engine-cooling equivalence ratio.

Trajectory

A three-degree-of-freedom model is used to compute flight trajectory, using the equations of motion of a point-mass aircraft moving relative to a rotating, spherical Earth. The trajectory flight path is computed using one of two methods.[15] First, an energy-state approximation is used, coupled to an input schedule of Mach number vs altitude. The second method is to specify a set of control variables (consisting of angle of attack, bank angle, throttle setting, and gimbal angle) and then to solve the equations of motion, using a first-order Euler integration (subject to a set of flight-path constraints, including maximum load factor and/or surface-temperature limits at a specified body location). For either modeling method, the trajectory can be computed untrimmed or trimmed in pitch.

Structural and TPS Weights

As part of the aircraft structural weight, the items estimated are shell, walls, frames, tension ties, spanwise beam, nonoptimum, and tank. The nonoptimum weight accounts for noncalculable weight items, such as fasteners, welds, cutout reinforcement, surface attachments, nonuniform gauge requirements, and manufacturing constraints and is a percentage of the preceding five weight items.

The tank item is an estimate of the weight of a discrete tank or of bulkheads and other items necessary to convert the body structure into an integral fuel tank. An option for noncircular vehicles is an integral, pillow-tank arrangement in which intersecting circular shells are fitted within the vehicle outer mold line.

The body-structural-weight-estimation method in the HAVOC is based on one-dimensional-beam theory structural analysis, resulting in a weight estimate that is directly driven by material properties, load conditions, and vehicle size and shape and is not confined to an existing database. Because the analysis is done station-by-station, along the vehicle longitudinal axis, the distribution of loads and vehicle geometry is accounted for, providing an integrated weight that accounts for local conditions.

The analysis begins with calculation of vehicle loads. Three types of loads are considered, longitudinal acceleration, tank pressure, and bending moment. Four loading cases are computed, power-on/tanks full, power-off/tanks full (abort condition), power-on/tanks empty (MECO condition), and power-off/tanks empty (entry condition).

It is assumed that structural materials exhibit elastoplastic behavior. The values of properties used are a reduced percentage of published, minimum values to account for such effects as fatigue, stress corrosion, creep, and thermal cycling, and thermal stresses that are not modeled as cold structures are considered.

The body weight analysis as described has been extensively correlated. It has been applied to existing aircraft for the purpose of determining the nonoptimum portion of structural weight. It has also been compared with many other analyses of hypersonic aircraft. For example, it was applied to the designs developed by the five prime contractors for the first aircraft concept downselect in the NASP program, and agreement was found to be generally excellent.

Estimation of TPS weight is based on transient, one-dimensional heat-conduction analysis. The aerothermal environments are computed as a function of time along the flight trajectory, including the recovery enthalpy, the enthalpy-based convective film heat transfer coefficient, and the local surface pressure for each surface panel. The one-dimensional materials stackup is specified for each body point, with associated internal boundary conditions, for example, internal gas bulk temperature and film coefficient, and internal radiation gap conditions input as function of time. Soak-out boundary conditions are also specified. Material thermoproperties are specified as a function of temperature and pressure (if applicable). The energy balance at the exterior surface is computed using a temperature-dependent emissivity for the corresponding TPS material. The TPS sizing process then consists of iterating on the required insulation thickness until all interior bondline temperature constraints are satisfied. Minimum-gauge TPS thickness constraints are also imposed.

The weight and volume of the vehicle subsystems are computed using correlation equations developed for space-launch and hypervelocity vehicles. Correlation parameters typically used related to overall vehicle gross or empty weight, vehicle size, and mission-related requirements. Correction factors for each subsystem element are made available to match a specifically known subsystem component weight. The accounted subsystem elements are flight controls and actuation (electrical, hydraulic and pneumatic), power generation and distribution, environment and life-support, thermal control, and propulsion-feed systems.

Life-Cycle Costs

The life-cycle cost (LCC) is based on airframe and engine development, vehicle acquisition, and operational costs. Cost-estimating relations are based on previous airplane programs, and these relations are supplemented, when necessary, to account for the fact that spaceplanes approach, rather than actually have, aircraftlike operation. The following databases were used: B-727, B-737, B-747, and B-757 (modified with those for X-15 and XB-70), engine,[16] launch vehicles (other than the space shuttle), and operations (airlinelike). Dry weights and vehicle speed are largely used for estimating development and acquisition costs. In the final analysis, the total cost of space operations (including procuring and launching a spacecraft) must be reduced.

Note that the cost-estimating relations for new vehicles, based on new technologies and new operating procedures, are likely to produce large uncertainties in the estimated costs. However, the same cost-estimating relations are used for all vehicles. The relative differences are, therefore, much less uncertain than the absolute costs.

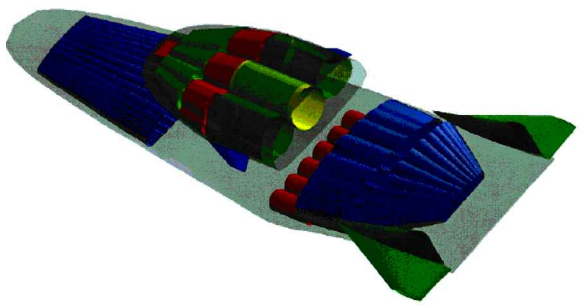

Fig. 5 Integral tanks.

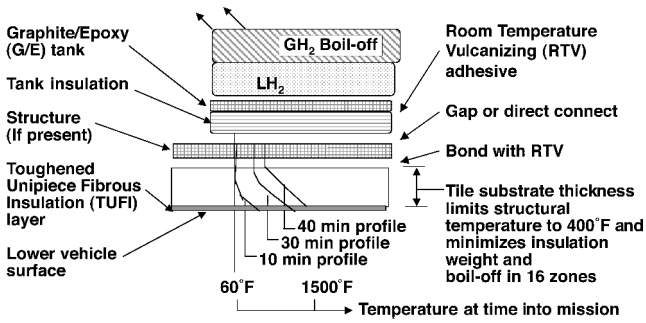

Fig. 6 TPS.

Hot vs Cold Structures

The launcher is modeled using 20 structural sections, with skins, stringers, and frames sized for bending, axial, and pressure loads. Liquid hydrogen tanks are integral tanks having intersecting lobes. Lobed tanks (Fig. 5) are also designed for bending, axial, and pressure loads. Liquid hydrogen tanks are made of graphite/epoxy (G/E) structure with Z-stiffeners, and with external Rohacell foam structure attached using polyurethane adhesive (Fig. 6). Toughened, unipiece fibrous insulation (TUFI) ceramic tiles are attached to the Rohacell foam tiles using room-temperature vulcanizing (RTV) adhesive and a Kapton® vapor barrier. Insulation thickness is sized for 16 zones, consisting of 20 perimeter points at 20 cross-sectional stations.

LOX tanks on the orbiter are Z-stiffened, aluminum–lithium tanks, with a similar TPS. The leading edges of the spaceplane have the same TPS as those assumed for the X-30 spaceplane. Engine surface unit weights and seals and systems weights are also derived from those for X-30.

The X-33 was designed with cold structures. It has load-carrying tanks and an external, leeward aeroshell and windward frame structure that supports the metallic, standoff TPS and transmits aerodynamic loads into the primary structure. The proposed TSTO spaceplane has directly bonded TPS.

Extensive development efforts during the 1960s through the 1980s on integrated thermal structures, for example, with titanium matrix composite (TMC) aeroshell, resulting in hot structures, have not demonstrated an advantage over cool structures, with external insulation, in terms of safety, robustness, risk reduction, and simplicity. Hot structures are heavy, complex, and expensive, particularly when structures are actively cooled.

Systems analyses for the launcher with Mach 5 staging and 25,000-lb payload indicate that the best structural approach for lightweight spaceplanes is using external TPS on a cool structure (Figs. 7 and 8). For these analyses, structures are constructed using G/E or aluminum (AL) alloys, and the external insulation of these structures is tailorable advanced blanket insulation (TABI), TUFI-8, or TUFI-12, where 8 and 12 indicate the density of title substrate. The research, technology, development, and evaluation (RTD&E) cost estimates for G/E structures with external insulation are significantly lower than the cost estimates for hot structures (Fig. 9).

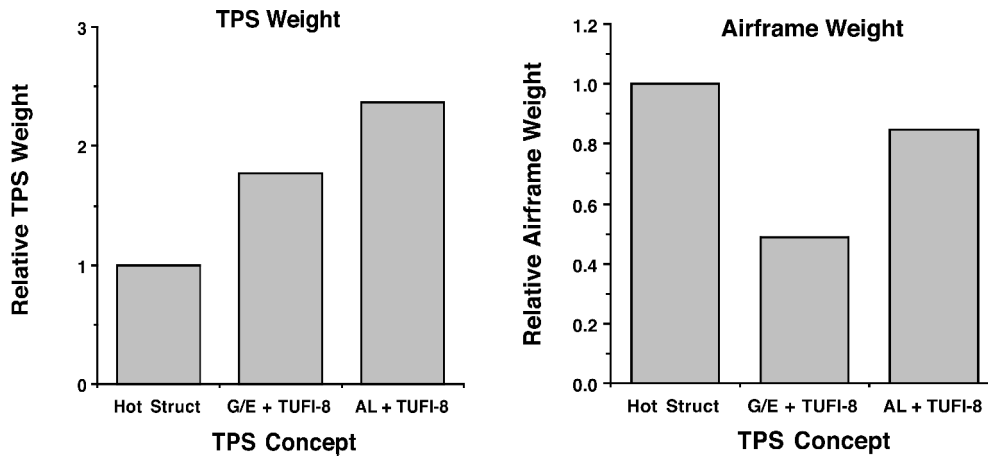

Fig. 7 Comparison of TPS weights and airframe weights for different TPS concepts.

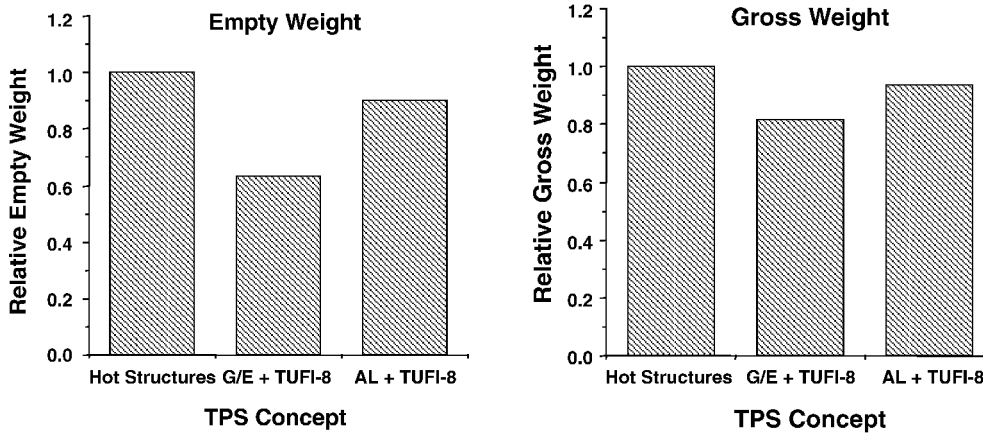

Fig. 8 Comparison of empty weights and TOGWs with different TPS concepts.

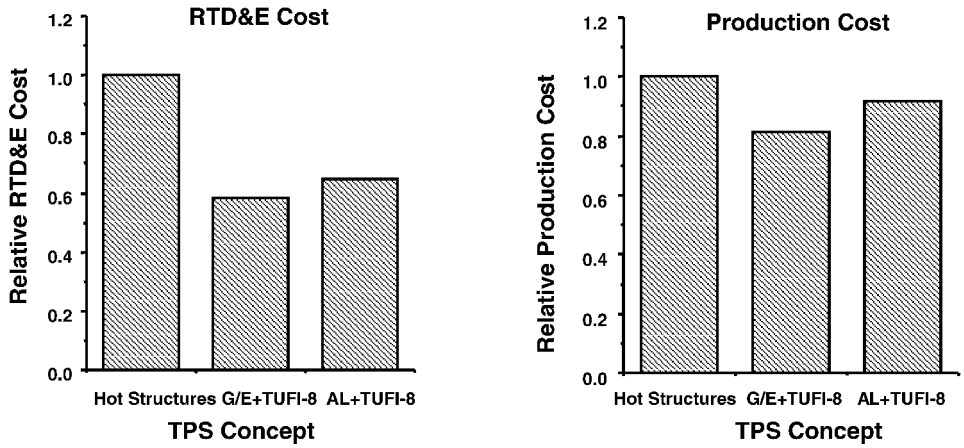

a) RTD&E and acquisition costs

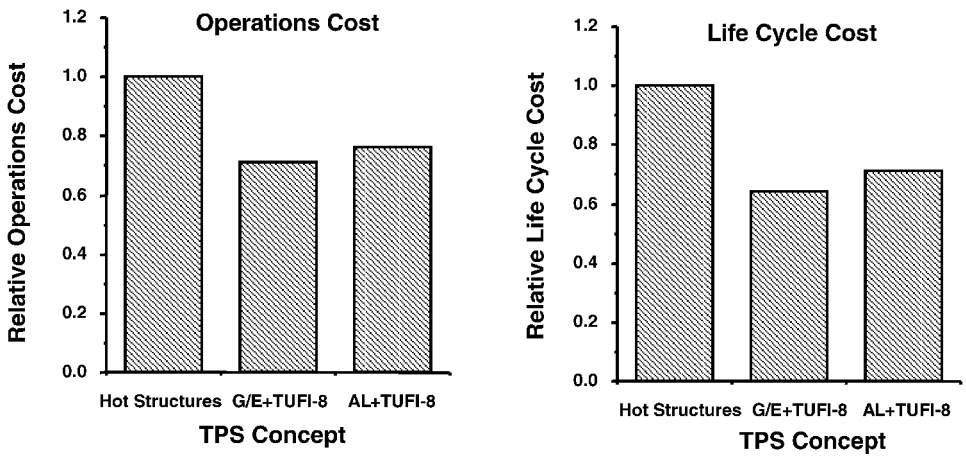

b) Operation and life-cycle cost

Fig. 9 Comparison of costs for different TPS concepts.

Subsequent to the hot vs cold study presented herein, the air-breathing/rocket SSTO group for the Access to Space–Advanced Technology Team also concluded that the use of external TPS on a cool structure leads to lighter spaceplanes.[17] In 2000, Langley Research Center, a member of the NASA Integrated System Analysis Team reported that cold, integral-tank structures were 23% lighter than hot-shell structures for hypersonic cruisers.

The external insulation design for spaceplane is lighter than those based on hot structures because 1) structures with low peak temperatures utilize more efficient and less expensive materials, 2) when the insulation is placed outside a structure rather than inside the structure, the usable volume of the structure increases, 3) the TPS is less complicated outside a structure compared to placing TPS under the outer surface of the structure, and 4) insulation of cryogenic tanks leads to a fewer requirements on TPS. Ceramic systems are generally lighter than metallic TPS as a result of relatively high attachment unit weight for metallic concepts, the latter becoming lighter only for high-integrated heat loads when expensive, lightweight multilayer insulation is used.

Installation of ceramic TPS on a cool structure, in turn, does impose design and integration issues on the airframe, including allowable strain constraints on the substructure for direct bond,

requirement for launcher panels in nonconformal tank regions, and surface shear and vibroacoustic limitations associated with blankets. Standoff metallic TPS does present integration issues, in terms of support structure, lower temperature limits, facesheet temperature gradient and thermal stress, and creep limitations. Metallic TP systems require multiuse coatings, which if damaged lead to chemical reactions due to catalysis and low emissivity at the metallic surface and may lead to a catastrophic failure. Both concepts require inspections and possibly maintenance work during operations.

Optimum Staging Mach Number

A study is conducted to assess the impact of the staging Mach number on the size, weight, performance, and LCC of the proposed TSTO spaceplane. The LCC is the least, if the staging Mach number is approximately Mach 10, as will be discussed.

As the staging Mach number is increased, the weight of the TPS increases on the launcher, increasing significantly above Mach 10 (Fig. 10), due to high, convective heat loads associated with high Mach and high-dynamic pressure-flight conditions. Likewise, the TPS fractions for the orbiter increase (but only slightly) because it is carried on the launcher, and entry heat loads primarily determine TPS weights. Apart from the harsher thermal environment at higher flight speeds, the size of the launcher slightly increases, with increasing fuel fractions (due, in part, to increased flyback fuel requirement), as the staging Mach number is increased. Empty weights of both stages decrease as the staging Mach number is increased, until Mach 12 (Fig. 11). Beyond Mach 12, the empty weight of the launcher increases, driven by the increased TPS weight and the increased structural weight as a result of higher, required mission-fuel fractions.

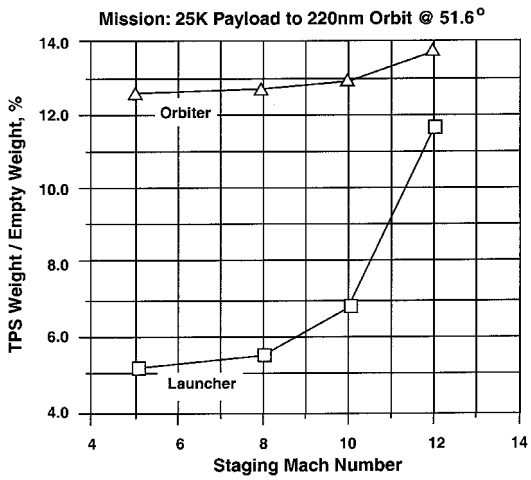

Fig. 10 Sensitivity of TPS weights to staging Mach number.

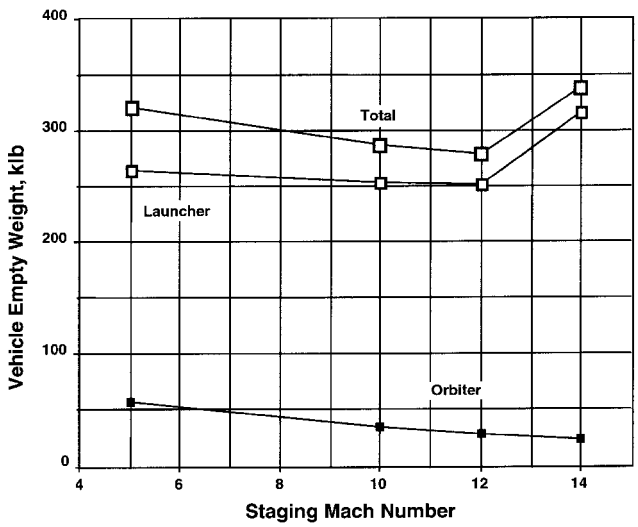

Fig. 11 Sensitivity of vehicle empty weight to staging Mach number.

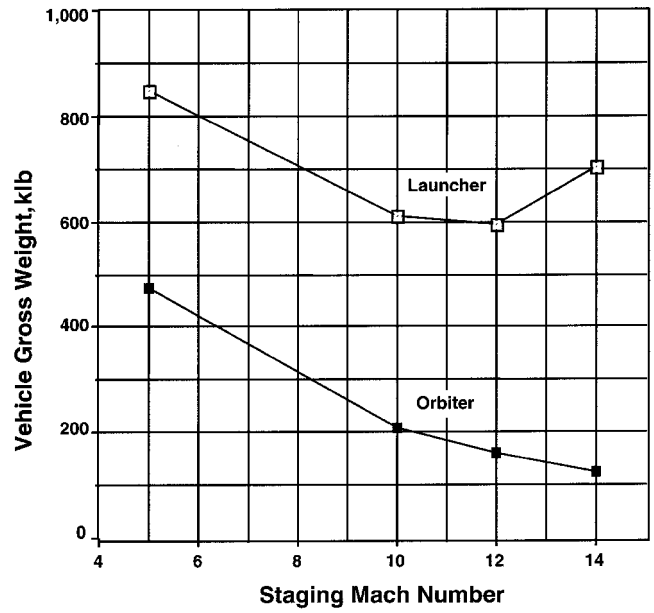

Fig. 12 Sensitivity of TOGW to staging Mach number.

As the staging Mach number is increased, the TOGW of the launcher decreases until Mach 12 (Fig. 12). The orbiter weight decreases because less fuel and oxygen are required for achieving reduced velocity increment to reach orbit with the higher staging Mach number. The launcher has to carry a lighter obiter, resulting in lower structural weights for the launcher because the fuselage bending moments are reduced. Thus, the total system weight is reduced for the same payload or the payload weight is increased for the same system weight, while the basic physical characteristics of the spaceplane remains the same as the staging Mach number is increased from 5 to 12.

When the Mach number is greater than 12, the required engine-equivalence ratio increases above the stoichiometric value to meet engine-cooling requirements, with an associated reduction in the engine-cycle specific impulse. This leads to higher mission-fuel fractions and, hence, higher closure gross weights. Finally, staging at a higher Mach number increases the downrange staging point, resulting in a longer cruise return to launch-site range requirement. This further increases the required mission fuel fraction and pushes the vehicle closure point to higher gross and empty weight values.

The RTD&E costs are driven primarily by subsystem weight or, in the case of the airframe RTD&E costs, by a dry-weight-speed product. The acquisition cost is primarily determined by dry weights, and operational costs are largely determined by maintenance and propellant costs. Maintenance costs are primarily a function of subsystem dry weight and vehicle surface area.

Figure 13 shows that the LCC decreases as the staging Mach number is increased, from Mach 5 to 10. From Mach 10 to 12, RTD&E costs of the launcher offset the reduced empty weight trend, resulting in increasing LCC. The cost of RTD&E and acquisition of scramjet engines, operating above Mach 10, increases.

Figure 14 shows the general configuration layout and dimensions of a typical spaceplane for Mach 10 staging. In Table 2, the lengths of the Mach 5 launcher and Mach 10 launcher are 224.5 ft and 221.5 ft, respectively. The lengths of the Mach 5 orbiter and Mach 10 orbiter are 75.5 ft and 72.7 ft, respectively.

Table 2 presents some details of mass properties for two spaceplanes, 1) the launcher and the orbiter for Mach 5 staging and 2) those for Mach 10 staging. In Table 2, the weights for the horizontal and vertical tails of the launcher are book kept under control surfaces. The payload for the launcher consists of the full-up orbiter launch weight, plus integration/separation-system increment. Subsystem dry weights include 15% weight margin. When it is assumed

Table 2 Mass properties for Mach 5 and Mach 10 spaceplanes

	Mach 5 staging		Mach 10 staging	
Item	Launcher, lb	Orbiter, lb	Launcher, lb	Orbiter, lb
Airframe	113,695	30,703	110,984	19,404
Wing and Tail	0	1,652	0	621
Fuselage	68,264	12,545	65,769	7,588
Fuselage TPS	15,271	8,371	18,103	5,621
Control Surfaces	18,217	4,813	17,059	3,758
Landing Gear	11,943	3,322	10,052	1,816
Propulsion	133,914	17,011	125,858	9,296
Ramjets or Ramjets and Scramjets	41,563	0	39,179	0
Rockets	0	12,088	0	6,605
Turbojets	69,181	0	65,175	0
Inlets	14,748	0	13,828	0
Fuel systems	8,233	4,924	7,675	2,691
Fixed equipment	17,269	9,689	14,405	4,535
Empty weight	264,879	57,403	251,247	33,235
Useful load	3,978	1,568	3,492	1,153
Consumables	1,176	1,083	1,759	801
Propellant	102,331	389,114	157,840	143,603
Payload	476,490	25,000	204,813	25,000
Gross weight	848,896	474,168	619,151	203,792

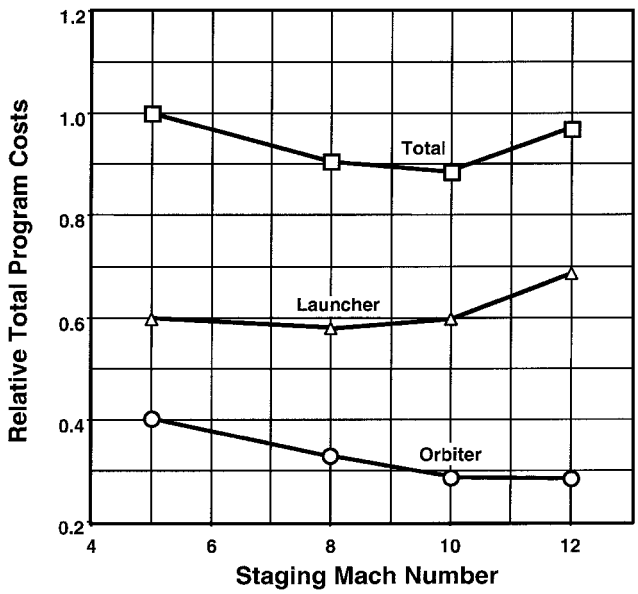

Fig. 13 Sensitivity of LCC to staging Mach number.

that the landing gear is made principally from TMC, its weight is aggressively assumed to be approximately 1.5% of the TOGW. The takeoff thrust-to-weights of the Mach 5 launcher and of the Mach 10 launcher at takeoff from 2306-ft elevation are 0.516 and 0.625, respectively. The Mach 5 TSTO vehicle is heavier than the Mach 10 TSTO vehicle, mainly because the orbiter of the former is heavier than of the latter. The overall trends presented in Figs. 10–12 are expected to be the same, even if some system weights were computed differently.

Essentially, the same airframes can be used for staging from Mach 5 through 10, with modest TPS weight difference. A basic design of a Mach 5 staging launcher is slightly modified to stage the orbiter at higher Mach numbers, or a launcher designed to stage at Mach 10 is used for launching the orbiter at lower Mach numbers. Likewise, an orbiter designed to stage at Mach 5 is slightly modified to stage at higher Mach numbers, or it is designed to stage at Mach 10, and used for staging at lower Mach numbers. Different combinations of the launcher and orbiter will lead to different payload launch capabilities. The combination giving the lowest LCC and highest growth potential requiring the least modifications is the one recommended.

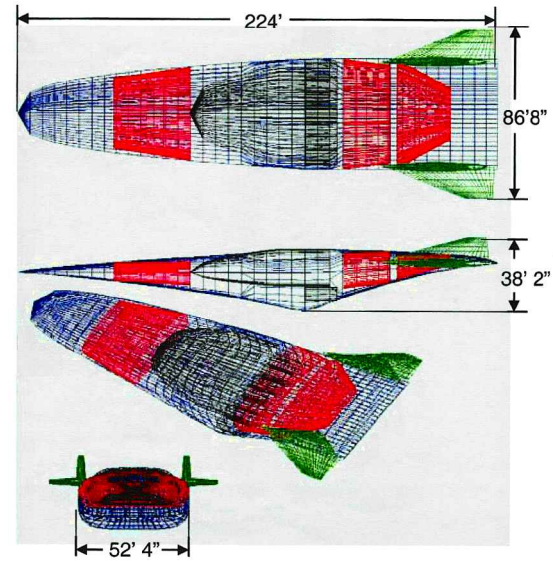

a) Launcher

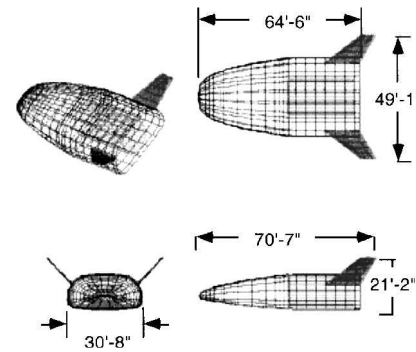

b) Orbiter

Fig. 14 Typical dimensions of TSTO spaceplane, M_{st} = 10:.

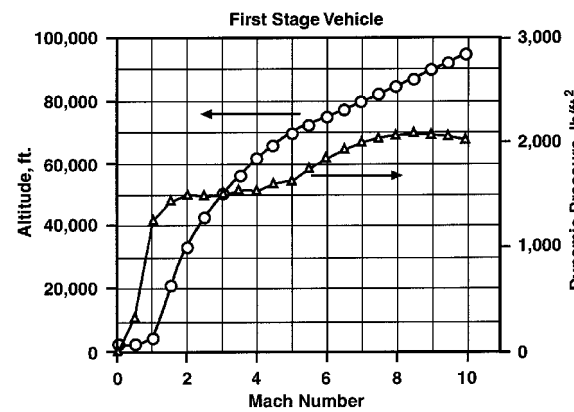

Fig. 15 Trajectory and dynamic pressure experienced by the launcher.

Performance at Mach 10 Staging

The flight trajectory of the spaceplane with a 25,000-lb payload during ascent is a typical airplane/airbreathing-type trajectory with an initial, low-speed acceleration at low flight-path angle (Fig. 15). The transonic flight regime is flown at an approximate dynamic pressure of 1250 lb/ft^2 to reduce the induced aerodynamic drag at the transonic minimum acceleration or pinch point. The dynamic pressure is about 1500 lb/ft^2 from Mach 2 to 4 for supersonic climb. Subsequently, the dynamic pressure is gradually increased to approximately 2100 lb/ft^2 during acceleration at hypersonic speeds. The relative cycle specific impulse and vehicle specific impulse from Mach 3 to 10 are presented in Fig. 16 for the launcher.

A 2.0-g pullup maneuver is initiated at Mach 10 and at an altitude of 95,000 ft, to lower dynamic pressures and to achieve the optimal

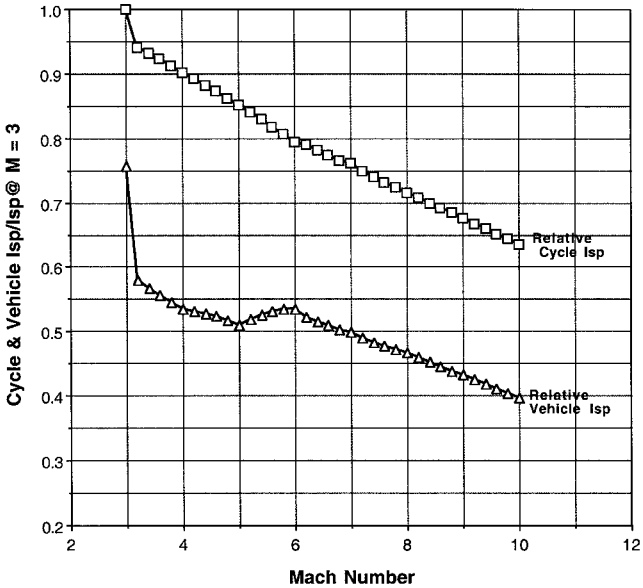

Fig. 16 Cycle specific impulse and vehicle specific impulse.

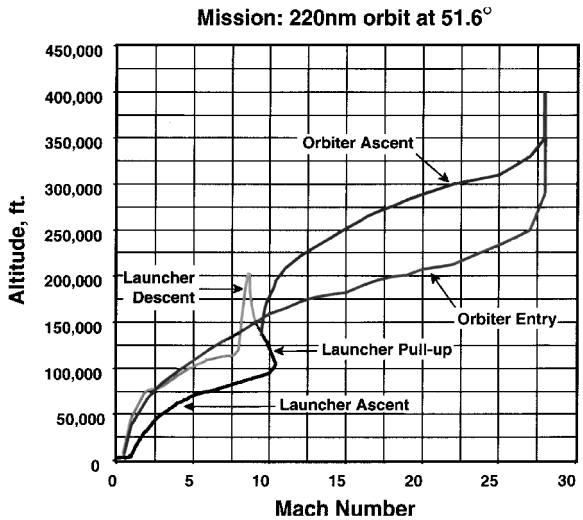

Fig. 17 Launcher and orbiter trajectories.

launching flight-path angle for the orbiter vehicle (Fig. 17). The MECO is at Mach 10.4 and at an altitude of 106,000 ft. The orbiter is launched at an altitude of approximately 140,000 ft and the dynamic pressure of 300 lb/ft^2. After second-stage separation, the launcher continues its unpowered ascent and initiates a 66.4-deg bank to begin the return-to-launch-site maneuver. Maximum attained altitude is approximately 200,000 ft. During entry, a turn to the cruiseback heading angle is completed, and the launcher cruises at maximum specific-range Mach number (2.0), using the low-speed turbojets to return to its launch site. The orbiter rapidly climbs and accelerates to approximately Mach 27.5, when it reaches the MECO condition, and then coasts to the desired orbit. Figure 17 also shows the orbiter entry flight. It uses low, initial-entry flight-path angle to ensure that heat loads are within the design margin.

A possible abort mission for the spaceplane consists of taking off, climbing, accelerating to the launch point, performing the pullup maneuver, and then aborting the launch and returning to the takeoff point (Fig. 18). When a decision is made to abort after MECO, and just before reaching the launch point, the spaceplane begins a roll to 66.4 deg, reaches maximum altitude of 206,000 ft at Mach 8.76, and then begins to descend. During atmospheric entry, the spaceplane experiences maximum dynamic pressure of 730 lb/ft^2 at Mach 7.5 and at an altitude of 106,000 ft. It reaches the maximum down range at Mach 6.4 and an altitude of 111,000 ft. After completing the U

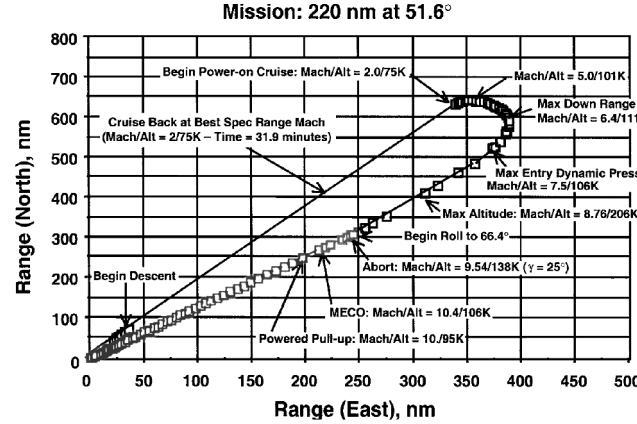

Fig. 18 Spaceplane launch, abort, and recovery ground track.

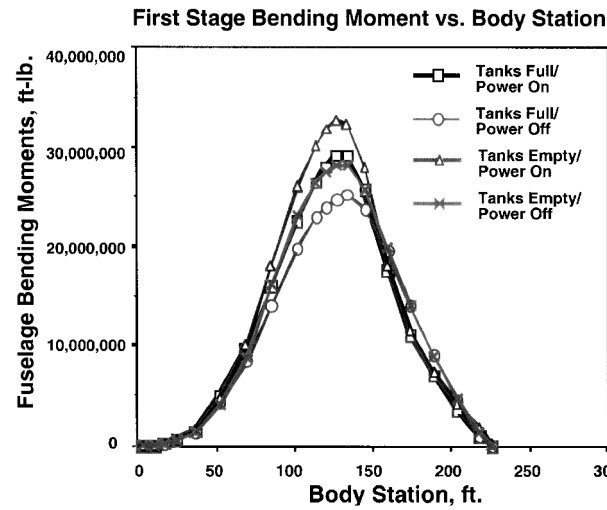

Fig. 19 Launcher bending moments.

turn, at normal loads less than 2.5 g, it is traveling at Mach 2 and is at an altitude of 75,000 ft. At this point, it begins turbojet power-on cruise back to the takeoff point at the best specific range Mach number. During the abort phase, the launcher continues to carry the orbiter at its full launch weight.

If a launcher engine shuts down at any point during the trajectory, the spaceplane can return safely to the airport of origin as would an airplane. The launch–abort mission impacts the sizing of the TPS and fuel load on the launcher.

The bending moment distributions on the launcher are shown in Fig. 19 for power-on/tanks full, power-off/tanks full (abort condition), power-on/tanks empty (MECO condition), and power-off/tanks empty (entry condition). For all loading conditions, the launcher is carrying the orbiter at its launch weight. Bending moments are distributed fairly symmetrically around the center of mass for all conditions.

Figures 20 and 21 show temperature time histories at specific, in-depth locations on the launcher and orbiter. Temperature histories at the surface, at the bondline between the external insulation and the internal cryogenic insulation, and at the interior surface of the internal cryogenic structures are plotted. The peaks in profiles for external surfaces are associated with peak heating environments encountered by these structures. The bondline temperature remains below 350°F, a design constraint. The resulting internal temperatures on the launcher's cryostructures are well below material allowable limits.

Prototype/Experimental Spaceplane with Builtin Growth

A TSTO spaceplane with Mach 5 staging offers lower performance at lower risk (because it avoids a scramjet), whereas that

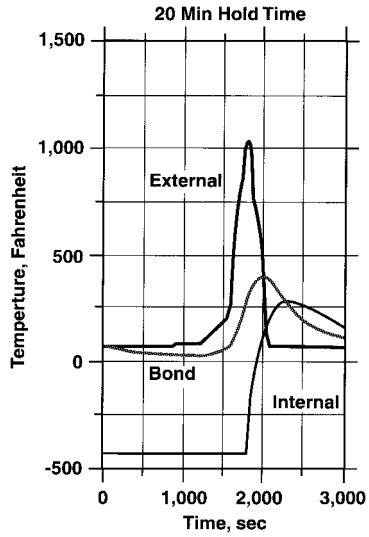

Fig. 20 Launcher surface and bondline temperature histories at 25 ft from the nose on the bottom surface.

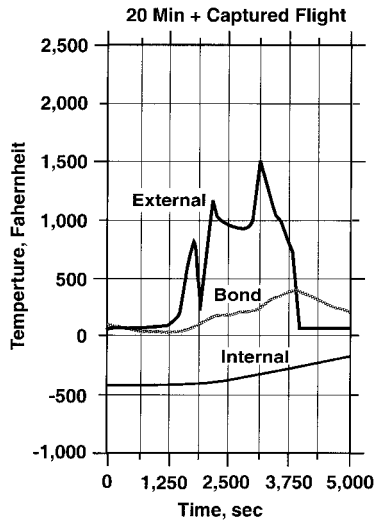

Fig. 21 Orbiter surface and bondline temperature histories at 25 ft from the nose on the bottom surface.

with Mach 10 staging offers higher performance at moderate risk (with a scramjet). Existing ground-test facilities and test techniques and subscale flight tests, such as those planned for X-43A (Hyper-X) at Mach 7 and Mach 10, are inadequate for developing full-scale, scramjet engines above Mach 8. As discussed in Ref. 10, new test facilities and techniques and flight tests with scramjet engines approaching those on spaceplanes are required, in the absence of at least two (preferably three) appreciably different size subscale engine tests.

These observations suggest the following programmatic philosophy.[10] First, a TSTO spaceplane is designed for Mach 10 staging to orbit with at least a 25,000-lb payload to the design orbit (51.6 deg and 220 n mile), the ISS resupply mission. Second, the spaceplane is used for space access by staging at Mach 6. (The reason for choosing Mach 6 rather than Mach 5 for staging is explained later in this section.) Third, a fully reusable rocket propulsion system is developed. Fourth, the launcher is used for demonstrating scramjet operations from Mach 6+ to 10. Fifth, once the scramjet is perfected to the level necessary and made operational, the spaceplane is used for space access by staging at Mach 10. Sixth, further development of scramjet technology at higher Mach numbers is conducted on a new, developmental second stage with an airbreathing flow path.

Following this philosophy, a prototype/experimental (P/X) TSTO spaceplane is recommended as a means of providing access to space, for developing the operational hypersonic airbreathing propulsion system, and for developing fully reusable rocket-propulsion system, with significantly improved mass fraction and margin.[10] In principle, the same plane may be a prototype plane and an experimental plane and could be called a growth plane.

The launcher is initially designed to achieve Mach 10. For example, the design of the launcher would include the TPS thickness distribution required to accommodate heat loads associated with Mach 10 operation and fuel tank capacity for the Mach 10 mission. The launcher airframe is a prototype. The launcher has a prototype propulsion system to achieve Mach 6 and has a demonstrator/experimental, dual-mode ram/scramjet engine from Mach 6+ to 10. The flow path of the experimental dual-mode ram/scramjet is the same as that for the prototype ramjet. The upper Mach 10 limit for the launcher is selected considering the staging Mach number trade study.

After an operational scramjet that can perform up to Mach 10 is developed, a block change of the prototype Mach 6 propulsion system and experimental Mach 10 engine to a prototype Mach 10, airbreathing propulsion system leads to a prototype launcher for Mach 10 staging.

Initially, orbiter-R is staged at Mach 6 because staging at Mach 6 reduces LCC from that for Mach 5 staging, while requiring little increase in the technology level for the launcher. The value of initial staging Mach number is chosen low to buildin payload growth to Mach 10, with the same launcher and the same orbiter-R.

The tanks on orbiter-R are sized for a Mach 6 launch. Consequently, orbiter-R would have excess propellant volume when launched at Mach 10 and may achieve higher altitude orbits than the design orbit with lighter payloads. At higher staging speeds, the tanks are partially filled for achieving design orbit, so that the eliminated propellant load is replaced by additional payload weight within the existing payload bay. Additionally, payloads with larger size could be accommodated by rearrangement of the internal propellant tank configuration.

Table 3 presents mass properties for the launcher designed to stage the orbiter at Mach 10, but initially stages the orbiter at Mach 6, and for the orbiter. The length of the launcher is 224.2 ft and that of the orbiter is 73.8 ft. The Mach 6 staged orbiter is capable of carrying a 8000-lb payload. The mass properties of this launcher are different from those for the Mach 10 launcher in Table 2, because these two launchers are designed differently.

Strategically, the next-generation transportation system should be put into service as soon as possible, even though, initially, it would transport payloads much lighter than 25,000 lb. If during the initial operations of this commonality spaceplane (with extra margins in the design and launching lightweight payloads) RTD&E are undertaken in flight, an early initial operational capability (IOC) can be achieved. As discussed later, the time saved in achieving early IOC saves billions of dollars in total launch costs.

The launcher and orbiter-R can be developed with a high level of confidence because vast amounts of data, information, and

Table 3 Mass properties for Mach 6 launch

Item	Launcher, $M_{st} = 10$, lb	Orbiter, $M_{st} = 6$, lb
Airframe	95,455	17,271
Wing and tail	13,725	2,732
Fuselage	55,124	7,263
Fuselage TPS	15,700	5,046
Control surfaces	2,448	819
Landing gear	8,458	1,401
Propulsion	126,477	7,174
Ramjets and scramjets	54,067	0
Rockets	0	5,097
Turbojets	49,609	0
Inlets	13,264	0
Fuel systems	9,536	2,077
Fixed equipment	14,007	6,329
Empty weight	235,939	30,773
Useful load	43,184	1,644
Consumables	1,409	779
Propellant	161,155	158,095
Payload	200,700	8,000
Gross weight	602,388	199,301

knowledge are available from low-speed systems, ramjet systems, the space shuttle orbiter, the NASP program, and other atmospheric-entry vehicles. Although the space shuttle main engine requires a major maintenance/overhaul after approximately four missions, data, information, and knowledge are available for building low-maintenance rocket engines that can be reused for approximately 15 missions without a major maintenance. (A few Russian rocket engines are claimed to achieve major-maintenance-free operations equivalent to approximately 10 missions.) The development of rocket engines that can be reused for approximately 50 missions, without major maintenance, will require technology efforts.

As discussed in Ref. 9, relevant technologies for all subsystems are low-risk technologies. For example, the ramjet was successfully ground tested to simulated Mach 8 conditions in the 1960s.

Because a significant portion of the evidence for establishing the credibility of the design would be direct evidence, the level of confidence in the design of the launcher would be quite high, to speeds of approximately Mach 6. The quantity of this type of evidence would decrease and the level of indirect evidence would increase as Mach 10 is approached. Also, the level of confidence in the design of orbiter-R, with major-maintenance-free rocket engines for approximately 15 missions, would be high.

The experimental scramjet engine on the P/X spaceplane would provide direct evidence in the Mach 6–10 range for developing a prototype ram/scramjet propulsion system. Initial flight experiences with orbiter-R would lead to the development of low-maintenance, 50-mission rocket engines.

Primarily, the integration of turbojet and ramjet engines, ramjet-scramjet transition, vehicle performance at low-hypersonic Mach numbers, stage separation, and the rocket propulsion system (with a 50-mission operability at low maintenance) are the risk items. These are relatively minor risks compared to the technical risk of developing a commercially viable, SSTO-R vehicle for IOC in 2012.

Since the access to space study,[8] hypersonic technologies have advanced, and new hypersonic technologies have been developed. Today, all required technologies for developing the proposed TSTO spaceplane that would stage the orbiter at Mach 6 with airbreathing propulsion on the launcher are believed to be at technology readiness level[8] (TRL) of at least 5. All TRLs can be brought to level 6 within 3–5 years.

Internal Rate of Return

Table 4 compares a spaceplane designed to stage at Mach 5 with a 25,000-lb payload on the orbiter and designated as the baseline spaceplane with a spaceplane (designated as the commonality spaceplane) whose orbiter is launched either at Mach 5 or 10. The baseline spaceplane is the same as that presented in Table 2. The TOGW of the commonality spaceplane and the weight of its orbiter are the same, whether the payload weight is 8,000 lb launched at Mach 5 or 41,000 lb launched at Mach 10. When the orbiter with a 25,000-lb payload is launched at Mach 10, the obiter's propellant tanks are not full.

Table 4 Weight and LCC comparisons of TSTO spaceplanes

Item	Baseline	Commonality
Payload, lb	25×10^3 at $M_{st} = 5$	8×10^3 at $M_{st} = 5$ 41×10^3 at $M_{st} = 10$
Weight, lb		
Launcher empty	265×10^3	255×10^3
Orbiter empty	57×10^3	41×10^3
Total empty weight	322×10^3	296×10^3
TOGW	849×10^3	751×10^3
Relative cost		
RTD&E	1.0	1.0
Acquisition	1.0	0.833
Operations	1.0	1.0
Total	1.0	0.96
Launch cost/lb	25×10^3 lb at 1.0	8×10^3 lb at 2.92 25×10^3 lb at 0.92 41×10^3 lb at 0.58

The commonality spaceplane and the P/X spaceplane stage orbiters with the same payload (8000 lb) at Mach 5 and Mach 6, respectively. The commonality spaceplane is heavier than the P/X spaceplane at takeoff (Tables 3 and 4), because the former stages at a lower Mach number than the latter. If the P/X spaceplane were designed to launch the orbiter with a 8,000-lb payload at Mach 6 and a 41,000-lb payload at Mach 10, then this spaceplane would be lighter than the commonality spaceplane.

The acquisition cost is for a fleet of five operational launchers and seven operational orbiters plus two ground-test vehicles, one for the launcher and one for the orbiter. For 22 years, 39 flights per year are operated. Cost estimates are in 1992 U.S. dollars.

The cost figures for the commonality spaceplane are referenced to those of the baseline spaceplane (Table 4). RTD&E cost for baseline spaceplane and for the commonality spaceplane is the same. The acquisition cost for the commonality spaceplace is 0.833% of that for the baseline spaceplane. The launch cost per pound of payload, for launching a payload weighing 25,000 lb, with the commonality spaceplane is approximately 0.92% of that for the baseline spaceplane.

The LCC for each of the three systems (all-rocket SSTO, airbreathing/rocket SSTO, and airbreathing plus all-rocket TSTO) considered under option 3 of the NASA access-to-space study[8] are almost the same as those for the other two systems (Fig. 22).

The TSTO spaceplane is a low-risk concept, requiring low-risk technology, compared to the SSTO rocket vehicle or the SSTO airbreathing/rocket vehicle. The sensitivity of the SSTO rocket vehicle to small changes in dry weight and in specific impulse is significantly larger than that of the TSTO spaceplane (Fig. 23) because the SSTO rocket has a very high fuel fraction requirement, approximately 90%.

A new launch vehicle meeting commercial requirements and interests must create profit to be a commercial success, that is, it should be economically viable. The RTD&E and acquisition costs of the new system, added to the overall costs of continued operation of the space shuttle and the existing fleet of expendable launch vehicles, leads to the increase in the launch vehicle total cost (Fig. 24). When a new fleet of reusable vehicles replaces a present fleet, the new fleet would greatly reduce operating costs.

The Mach 5–10 commonality TSTO spaceplane substantially reduces the need for experimental vehicles. Additionally, the commonality spaceplane, with early operations at $M_{st} = 5$, and with subsequent operations at $M_{st} = 10$ 1-year later, saves tens of billions of dollars over a 5-year period.[9] The TSTO commonality spaceplane

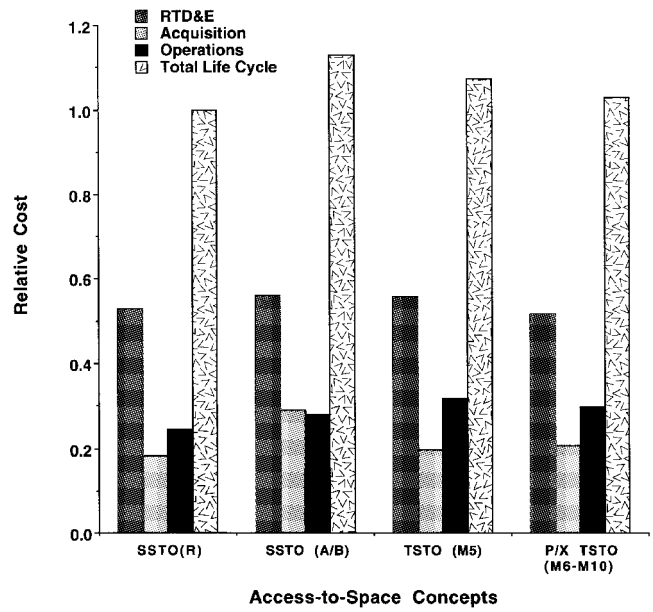

Fig. 22 LCC for the access-to-space study vehicles.

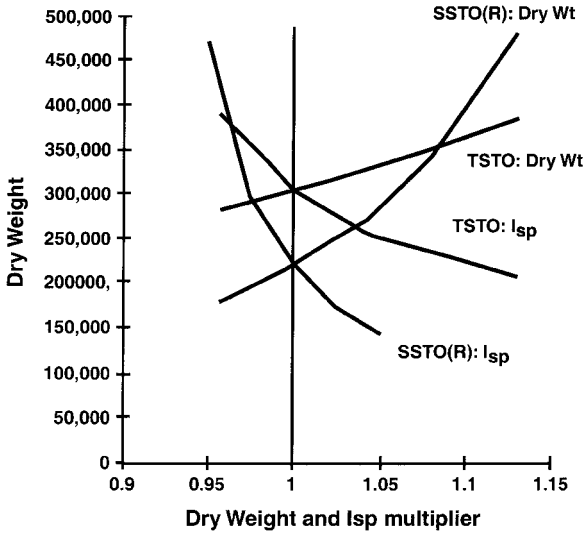

Fig. 23 Sensitivities of SSTO rocket-powered vehicle and TSTO spaceplane.[9]

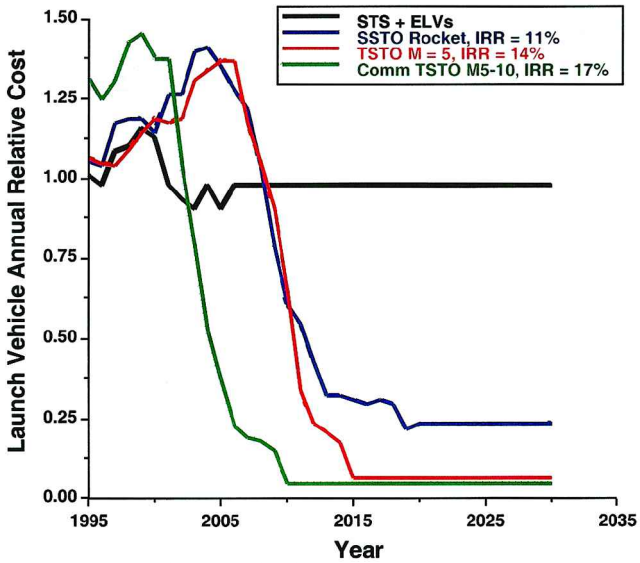

Fig. 24 Funding streams over time, with internal rate of return (adapted from Ref. 9).

achieves operational status much earlier than the SSTO rocket vehicle and the TSTO Mach 5 staging spaceplane because the latter vehicles are assumed to have a 5-year technology program, which includes flight demonstrations, to reduce risk. In the case of the commonality spaceplane, technology development and risk reduction are carried out in flight, whereas lightweight payloads are launched to reduce total launch costs.

A less aggressive program is the one proposed earlier for developing the P/X TSTO spaceplane. This program begins with a technology development effort to bring all technologies to TRL 6 before embarking on the development of this spaceplane. First, this spaceplane is made operational to stage at Mach 6. Next, a successful scramjet engine demonstration in-flight on the launcher is followed by a block change of the experimental engine to a prototype engine resulting in a prototype TSTO spaceplane capable of staging at Mach 10. The transition from Mach 6 to Mach 10 staging with an operational spaceplane is achieved quickly.

The internal rate of return (IRR) is computed considering the investment for developing a new system and the savings realized when the old systems are no longer used. The SSTO rocket system, the TSTO spaceplane with staging at Mach 5, and the commonality spaceplane were estimated to provide, respectively, 11, 14, and 17% IRR. The proposed P/X spaceplane is estimated to offer a 15% IRR. However, 17% IRR is not high enough for an economically viable launch system. A 20% return on investment may be feasible, if the first 2 years of the development program are publicly and substantially funded.[9]

The determination of IRR is done assuming that noncommercial and commercial mission requirements and interests for space access can be converged into a single spaceplane. It is difficult to make this assumption a reality. To converge noncommercial/commercial mission requirements and interests for space access into a family of TSTO spaceplanes is easy to achieve.

Further Growth Potential[10]

The principal scramjet development challenge is in the Mach 10–23+ range. Development of a prototype spaceplane leading to a fleet of operational vehicles requires 1) a demonstration of net scramjet thrust across the complete airbreathing hypersonic Mach number range of interest, 2) validation of simulation models and verification of simulation-design tools, and 3) verification in an actual vehicle of the technologies and systems required for such vehicles.

Three orbiters are developed (Table 5). The launcher and the orbiters are reusable, piloted, and land horizontally; the launcher takes off horizontally. The airframe and the turbo/ramjet on the launcher are fully reusable; the orbiter has fully reusable airframe and has low-maintenance rocket engines.

The three orbiters are 1) orbiter-R with an all-rocket propulsion cycle, 2) orbiter-E with a rocket/airbreathing propulsion system, and 3) orbiter-A with an airbreathing/rocket system. Orbiter-R is a prototype vehicle, designed to go to orbit. The launcher and orbiter-R make up the earlier proposed and discussed P/X TSTO spaceplane. Orbiter-E and orbiter-A are discussed herein.

The reusable and operationally flexible launcher provides vital access-to-space launch and hypersonic flight-test services capability. The orbiter-R provides short-term economical benefits by achieving orbit for space missions, whereas orbiter-E (Table 5) is used for further scramjet development. This orbiter serves as a testbed for conducting experiments and developments at high dynamic and heating loads, such as those related to full-scale structural panels and components, including scramjet engines. Orbiter-E is utilized as the X-7 and X-15 planes were. It may be piloted or unpiloted.

The Mach 5–24 range is divided into three ranges, low (from Mach 5+ to 10), moderate (from Mach 10+ to 18), and high Mach number (from Mach 18+ to 24) ranges. This division facilitates testing of the scramjet operation over the low-hypersonic Mach range, with the launcher and the incremental development of airbreathing propulsion with orbiter-E at moderate- and high-hypersonic Mach numbers. This divide-and-conquer philosophy significantly reduces development and flight-test risks.

Orbiter-E is designed to go from Mach 9+ to 24 and is primarily a rocket-powered vehicle with only one replaceable airbreathing engine. The orbiter is designed to fly, when required, selected parts of orbiter-A's airbreathing trajectory. The configurations of orbiter-E and orbiter-A may be different from that for orbiter-R.

The development of the airbreathing propulsion system with orbiter-E is accomplished in three steps of increasing technological challenges: from Mach 9 to 12, Mach 12+ to 18, and Mach 18+ to 24. Once this system is developed in the Mach 9–12 range, the prototype orbiter-A is built and/or the airbreathing range of the launcher is extended. When the scramjet is developed in the range from Mach 12+ to 18, the airbreathing range of orbiter-A is extended

Table 5 Characteristics of TSTO P/X spaceplane

Vehicle	Mach range	Propulsion[a]	Airframe
Launcher	0–6	Turbo/ram (P)	P
	6–10	Ram/scramjet (X)	
Orbiter-R	6–orbit	Rocket (P)	P
Orbiter-E	9–24	Rocket(O)/Scramjet (X)	P
Orbiter-A	9–orbit	Scramjet(P)/Rocket (O)	P

[a]P is prototype, X experimental, and O operational.

and/or the development of a prototype SSTO spaceplane with airbreathing/rocket propulsion is undertaken. Once the airbreathing propulsion system is developed in the range from Mach 18+ to 24, an airbreathing launcher is developed to launch the orbiter at Mach numbers in low 20s for high-energy orbits and/or the airbreathing range of SSTO is extended. Thus, the airbreathing component (scramjet) of the RBCC engine is further developed.

Orbiter-E is not built until the hypersonic propulsion system performs satisfactorily in the launcher, up to Mach 10, and is well understood. While the launcher and orbiter-R are designed, built, tested, evaluated, and made operational, a program is carried out for advancing the hypersonic facility capability and for improving appropriate, nonintrusive, flow-diagnostic technology applicable to the hypersonic environment. Flight-test data from flights of the launcher in the low-hypersonic Mach number range would improve computational-design technology and calibrate ground-test data. These advances and enhancements would help in the design of an experimental air-breathing propulsion flow path for orbiter-E, with a high level of confidence in its design. Flight tests of this truly experimental vehicle in the moderate and high Mach number ranges and the advances in hypersonic facilities would result in a high level of confidence in the design of orbiter-A.

Rocket and airbreathing propulsion options are pursued. These propulsion systems and the proposed vehicles open up, for example, the following further growth potentials and multiple avenues, any one of which may be pursued with a high level of confidence: 1) replacement of orbiter-R with orbiter-A, 2) development of an airbreathing/rocket SSTO vehicle, 3) development of an all-rocket SSTO vehicle, 4) development of a hypersonic globecruiser, 5) development of an unpiloted orbiter, 6) development of an expendable, unpiloted orbiter for high-energy orbits, 7) development of reusable orbiters for specific payloads, 8) development of a launcher for staging the orbiter at Mach 20–23 for geostationary orbit, and 9) development of a reusable TSTO spaceplane for lunar transportation.

Conclusions

The foremost objective is to reduce cost greatly and substantially improve safety and reliability for human exploration of space. In the near term, this objective can be best met using a TSTO concept with a TBCC propulsion system on the first stage.

Spaceplanes with low-risk technologies and builtin growth potential and aircraftlike operations provide the most return on investment. The proposed, conceptual TSTO spaceplane (P/X-spaceplane) is closest to meeting economic requirements, a 20% rate of return on investment, if noncommercial and commercial mission requirements and interests can be converged into a single spaceplane. The proposed spaceplane significantly reduces risk, increases margin, and maintains the SSTO option.

The P/X-spaceplane launcher assists the development of hypersonic airbreathing propulsion and meets the desired access-to-space requirements near term with an operational version. The orbiter assists in the development of long-life, low-maintenance rocket engines. This strategy offers a number of advantages, is technology driven, opens up multiple future avenues, provides short-term benefits, has builtin growth potential, and is achievable. The proposed TSTO spaceplane appears to be the correct choice for the development of the next-generation, reusable launch vehicles.

Acknowledgements

While at the NASP National Program Office, Unmeel B. Mehta advocated that the NASP program should set aside the SSTO requirement and develop a TSTO spaceplane with airbreathing propulsion on the first stage. Subsequently, Thomas J. Gregory directed at NASA Ames Research Center the development of the TSTO spaceplane concept for the NASA access to space study. The authors thank Thomas J. Gregory (retired), William D. Henline, and David J. Kinney, Howard E. Goldstein (retired) of NASA Ames Research Center, William J. D. Escher of Scientific Applications International Corporation, and Henry G. Adelman of Eloret Corporation for their helpful comments and suggestions when they reviewed the manuscript of this paper. The authors also appreciate the comments, questions, and suggestions provided by the reviewers for the *Journal of Propulsion and Power*.

References

[1]Augenstein, B. W., Harris, E. D., with Aroesty, J., Blumenthal, L., Brooks, N., Frelinger, D., Garber, T., Gottenmoeller, R., Hiland, J., Liu, S. K., Pace, S., Rosen, J., Rowell, L., and Stucker, J., "The National Aerospace Plane (NASP): Development Issues for the Follow-on Vehicle, Executive Summary," RAND, R3878/1-AF, Santa Monica, CA, 1993.

[2]Hallion, R. P., and Young, J. O., "Space Shuttle: Fulfillment of a Dream," *The Hypersonic Revolution*, Vol. 2, edited by R. P. Hallion, Special Staff Office, Aeronautical Systems Div., Wright–Patterson AFB, OH, 1987.

[3]"National Aero-Space Plane, Restructuring Future Research and Development Efforts," Rept. NSIAD-93-71, U.S. Government Accounting Office, 1993.

[4]Rich, B. R., and Janos, L., *Skunk Works: A Personal Memoir of My Years at Lockheed*, Little Brown and Co., Boston, MA, 1994.

[5]Dornheim, M. A., "Engineers Anticipated X-33 Tank Failure," *Aviation Week and Space Technology*, Vol. 151, No. 20, 1999, pp. 28–30.

[6]"Final Report of the X-33 Liquid Hydrogen Tank Test Investigation Team," NASA George C. Marshall Space Flight Center, May 2000.

[7]Bekey, I., "Forget About Shuttle Upgrades, Go With RLVs," *Aviation Week and Space Technology*, Vol. 152, No. 17, 2000, p. 82.

[8]"Access to Space, Advanced Technology Team Final Report," Vol. 1, Executive Summary, NASA, CN-162499, July 1993.

[9]Gregory, T., Bowles, J., and Ardema, M., "Two-Stage-to-Orbit Air-Breathing and Rocket System for Low Risk, Affordable Access to Space," *Journal of Aerospace*, Sec. 1, Vol. 103, 1995, pp. 189–201; also Society of Automotive Engineers, SAE Paper 94-1168, April 1994.

[10]Mehta, U. B., "Strategy for Developing Air-Breathing Aerospace Plane," *Journal of Aircraft*, Vol. 33, No. 2, 1996, pp. 377–385; Errata, Vol. 33, No. 4, 1996, p. 840. (This paper is an updated and shortened version of "Air-Breathing Aerospace Plane Development Essential: Hypersonic Propulsion Flight Tests (Invited)," *Proceedings of the 2nd European Symposium on Aerothermodynamics for Space Vehicles*, ESTEC, Noordwijk, The Netherlands, 21–23 November 1994, ESA SP-367, February 1995.)

[11]Morris, R. E., and William, N. B., "A Study of Advanced Air-Breathing Launch Vehicles with Cruise Capability," Vols. 1–4, NASA CR 73194-73199, 1968.

[12]Novichov, N., "At Hypersonic Speeds," Foreign Aerospace Science and Technology Center, Rept. FASTC-ID(RS)T-0972-92, Wright–Patterson AFB, OH, 1993; translated from *Ekho Planety*, Vol. 42, No. 237, 1992, pp. 4–8.

[13]Faye, J. A., and Riddell, F. R., "Theory of Stagnation Point Heat Transfer in Dissociated Air," *Journal of Aerospace Sciences*, Vol. 25, No. 121, 1958, pp. 54–67.

[14]Lee, L., "Laminar Heat Transfer over Blunt Nosed Bodies at Hypersonic Flight Speeds," *Jet Propulsion*, Vol. 26, No. 4, 1956, pp. 259–269.

[15]Windhorst, R., Ardema, M., and Bowles, J., "Minimum Heating Entry Trajectories for Reusable Launch Vehicles," *Journal of Spacecraft and Rockets*, Vol. 35, No. 5, 1998, pp. 672–682.

[16]"Hypersonic Research Facilities (HyFAC) Study," Vol. 5, NASA CR 114330, 1970.

[17]Hunt, J. L., "Airbreathing/Rocket Single-Stage-to-Orbit Design Matrix," AIAA Paper 95-6011, 1995.